ORIGINAL ARTICLE

ETRI Journal WILEY

MLCNN-COV: A multilabel convolutional neural network-based framework to identify negative COVID medicine responses from the chemical three-dimensional conformer

Pranab Das | Dilwar Hussain Mazumder

Department of Computer Science and Engineering, National Institute of Technology Nagaland, Dimapur, India

Correspondence
Dilwar Hussain Mazumder, Department of Computer Science and Engineering, National Institute of Technology Nagaland, Dimapur, India.
Email: dilwar2k4@yahoo.co.in

Abstract

To treat the novel COronaVIrus Disease (COVID), comparatively fewer medicines have been approved. Due to the global pandemic status of COVID, several medicines are being developed to treat patients. The modern COVID medicines development process has various challenges, including predicting and detecting hazardous COVID medicine responses. Moreover, correctly predicting harmful COVID medicine reactions is essential for health safety. Significant developments in computational models in medicine development can make it possible to identify adverse COVID medicine reactions. Since the beginning of the COVID pandemic, there has been significant demand for developing COVID medicines. Therefore, this paper presents the transfer-learning methodology and a multilabel convolutional neural network for COVID (MLCNN-COV) medicines development model to identify negative responses of COVID medicines. For analysis, a framework is proposed with five multilabel transfer-learning models, namely, MobileNetv2, ResNet50, VGG19, DenseNet201, and Inceptionv3, and an MLCNN-COV model is designed with an image augmentation (IA) technique and validated through experiments on the image of three-dimensional chemical conformer of 17 number of COVID medicines. The RGB color channel is utilized to represent the feature of the image, and image features are extracted by employing the Convolution2D and MaxPooling2D layer. The findings of the current MLCNN-COV are promising, and it can identify individual adverse reactions of medicines, with the accuracy ranging from 88.24% to 100%, which outperformed the transfer-learning model's performance. It shows that three-dimensional conformers adequately identify negative COVID medicine responses.

KEYWORDS
chemical three-dimensional conformers, convolutional neural network, COVID medicine development, negative medicine reactions, transfer-learning

1 | INTRODUCTION

During the first half of 2020, the World Health Organization declared COronaVIrus Disease (COVID) as a pandemic all over the world [1, 2]. As of early September 2022, more than 590 million confirmed cases of COVID, and more than 6.5 million people had died. Every day, the number of COVID positivity and death increases rapidly and continuously. So, effective COVID medicines are necessary to cure this disease [3]. Negative medicine responses are unwanted, adverse, and unfavorable effects. Because of COVID, global public health will face significant problems and health concern issues in the near future [4–6], so the development of effective medicines (drugs) is essential. Predicting adverse COVID medicine reactions is critical to the medicines development pipeline. Also, one of the most common reasons for medicine failure is harmful medicine reactions. Therefore, predicting the adverse COVID medicine reactions is needed for human health concerns. Several computational models are available for medicines development, design, and discovery. In the current work, MobileNetv2, ResNet50, VGG19, DenseNet201, Inceptionv3, and MLCNN-COV have been employed to identify negative responses of COVID medicines.

In the early phase of medicines development, discovery, and design, medicines properties play a crucial role in analyzing negative medicine responses [7]. While many pharmacological features have been used to predict negative medicine responses to analyze various medicines, chemical 3D conformers have yet to be applied to predict adverse COVID medicine reactions. The one-dimensional chemical structure, medicine-like properties, medicines functions, and biological characteristics (protein and gene expression signature) of medicines have been utilized in most of the research work on medicines discovery, development, and design to identify adverse medicine reactions [8–11]. However, the image of the three-dimensional chemical conformers may be crucial for predicting negative medicine responses because negative responses of medicines may be related to chemical conformers' structures. The research community has not yet used computational methods to investigate the association between three-dimensional chemical conformers and adverse medicine reactions. The problem of pessimistic medicine response prediction using a chemical three-dimensional conformer structure is multilabel since there may be numerous adverse reactions that correspond to a given medicine.

The key contribution of this study is presenting a framework with an image augmentation technique for predicting adverse medicine reactions via designing an MLCNN-COV from the properties of the three-dimensional chemical conformer that have not yet been used to predict negative responses of COVID medicines. Also, a multilabel pretrained models framework is presented to compare the performance of MLCNN-COV.

The remaining sections of this article have been arranged as follows: the next section summarizes related work to identify negative responses of medicines. The following sections demonstrate the dataset, suggested MLCNN-COV methodology, and other transfer-learning models. After that, the experimental design and outcomes have been provided. The last section summarizes the conclusions of the work.

2 | RELATED WORK OF NEGATIVE MEDICINE RESPONSE

In their work, Das and others [9] analyze adverse medicine (drug) responses from the medicine functions. To perform the experiments, the authors applied the binary relevance transformation method with the help of extra tree classifier (ETC), random forest (RF), K nearest neighbors (KNN), decision tree (DT), and multilayer perceptron neural network (MLPNN). They obtained that ETC classifiers results outperformed the other machine learning methods. In a different work, Das and others [8] utilized medicine functions, 17 molecular properties, and simplified molecular input line entry system (SMILES) and their combination to identify negative medicine responses. Further, the authors applied deep neural network (DNN) in all integrated medicine properties datasets. They found that the combination of SMILES string and medicines functions exhibits better results than other medicine properties. Wang and others [11] detected negative responses of medicine from biological information, biomedical literature information, and 17 molecular properties. The authors presented a DNN model to identify negative medicine responses. Further, they compared the DNN model with Gaussian Naïve Bayes (GNB), linear support vector machine (SVM), and probabilistic matrix factorizer models and found their proposed model performs well. Istswaart and others [12] applied RF and analyzed the association between pharmacovigilance assay properties and negative medicine responses. Further, antidepression adverse medicine reactions are identified by Gunes and others [13] from transporters, medicine-target, chemical structure, and enzyme. They applied multilayer perceptron (MLP), SVM, and KNN to execute their experiment and found that the MLP method outperformed the other classifier approaches. Shankar and others [14] presented an artificial neural network (ANN) model to predict medicine pair harmful reactions from the chemical structure and gene expression.

The COVID vaccine negative responses are analyzed by Hatmal and others [15] from the online survey and applied XGBoost, RF, MLP, and K-Star and found that RF performs well than other machine learning methods. Swathi [16] predicts adverse medicine reactions from the medical health form and applied linear regression (LR), DT, RF, Naïve Bayes (NB), SVM, and linear support vector classifier (LSVC) and found that RF outperforms than other computational methods. In Jamal and others [17], a RF and sequential minimization optimization computational methods are applied to identify negative cardiovascular medicine responses from phenotypic, biological, and chemical structures, and they found that phenotypic properties are better than the other properties. In a different work, Jamal and others [18] employed SVM and detected negative responses of neurological medicine from phenotypic, biological, and chemical structures. They found that the combination of all the medicines properties performance is comparatively better than the other three-level, two-level, and individual medicines properties. An LR model is presented by Pouliot and others [19] to identify adverse medicine reactions from the system organ class. Further, an SVM computational learning model is presented by Liu and others [20] to analyze adverse medicine reactions from medical reports. In Jahid and Ruan [21], an ensemble method is provided to identify adverse medicine reactions from chemical structure. Jiang and Zheng [22] utilized Twitter posts to detect negative medicine responses by employing SVM, NB, and maximum entropy (ME). Their presented ME method obtained good results comparatively than others. An SVM model is applied by Huang and others [23] to identify potential negative medicine responses from protein–protein interactions, medicine-target, and chemical structure. In LaBute [24], an LR model is presented to detect negative medicine responses from protein-target. Zhang and others [25] provided an FSMLKNN classifier approach to detect negative responses of medicine from chemical and medicine-target properties. Further, a machine learning methodology is presented by Niu and others [26] by utilizing kernel regression (KR), SVM, neural network (NN), and sparse canonical correlation analysis (SCCA) to detect adverse medicine reactions. Hu and others [27] proposed a novel approach GraphSE to predict negative medicine responses from the medicines substructure. The authors compared their proposed model with SCCA, SVM, NB, GraphSE-NCut, and GraphSE-RankClus and found that their proposed approach achieved better results than the existing machine learning approaches.

A DNN model is proposed by Odeh and Taweel [28] to detect negative medicine responses from Twitter posts. Their proposed approach achieved the highest results compared with existing models such as recurrent convolutional neural network (RCNN), convolutional neural network (CNN), CNN with attention (CNNA), majority vote classifier, and CNN-Google News. In a different work, Wang and others [29] summarized the commonly used machine learning models and medicine properties to predict negative medicine responses and reviewed several research articles on pessimistic medicine response prediction. Nguyen and others [30] presented a brief description of machine learning techniques, medicine features, and pessimistic medicine response prediction tasks. The authors summarized negative medicine responses related to articles and analyzed their challenges and research gaps. Depth analyses of pessimistic medicine responses prediction and detection articles are summarized by Das and others [31] based on the different medicinal properties and computation approaches to predict negative medicine responses. Also, the authors analyze different problems and challenges during pessimistic medicine response prediction.

The negative medicine response prediction literature demonstrates how pharmaceuticals use transcriptomic data (gene expression information), medicine-target, biological information, and 1D chemical structure. According to the literature review, there is still necessity to make some improvements in the medicines discovery, development, and design, including utilizing unexplored medicine attributes to identify negative medicine responses, such as three-dimensional chemical conformers. The ability to identify negative COVID medicine responses from the three-dimensional chemical conformer has not yet been utilized. This work aims to design an MLCNN-COV and multilabel transfer-learning framework with an image augmentation technique to predict negative COVID medicine response by employing a three-dimensional chemical conformer.

3 | PROPOSED METHODOLOGY AND WORKFLOW OF THE FRAMEWORK

This section demonstrates the proposed MLCNN-COV and transfer-learning framework and the problem statement with the solution for predicting negative COVID medicine reactions from the image of a three-dimensional chemical conformer.

3.1 | Datasets description

The procedure of developing the Negative COVID Medicine Responses Dataset (CMRD) for the proposed framework to predict negative medicine responses from

the three-dimensional chemical conformer has been illustrated in Figure 1.

The drugs.com website lists several medications that can be used to treat COVID illness. Among those medicines, only 17 COVID medicines chemical three-dimensional conformer are listed in PubChem [32] such as Remdesivir, Umifenovir, MK-4482, Baricitinib, Colchicine, Dexamethasone, Favipiravir, Hydroxychloroquine sulfate, PF-07321332, Protein kinase inhibitors, Zyesami, Fluvoxamine, Hydroxychloroquine, Chloroquine phosphate, Peginterferon Lambda, Bemcentinib, and Methylprednisolone. After collecting the COVID medicine name from Drugs.com (Link: https://www.drugs.com/condition/covid-19.html?page_all=1), the three-dimensional conformers are collected from the PubChem data repository. The medicine name is utilized as input on the PubChem search space to collect three-dimensional conformers' images (Link: https://pubchem.ncbi.nlm.nih.gov/). After that, by clicking the medicine link, select the 3D Conformer section and choose the ball and stick chemical structure. Further, select the Get Image option, choose the Large size of the image, and download it. Furthermore, negative medicine responses for each drug are collected from WebMD (Link: https://www.webmd.com/). On the WebMD [33] website, 29 adverse medicine reactions are listed for those 17 COVID medicines, such as asthma attack, sweating, headache, liver function test abnormal (LFTA), weakness, blood pressure increased (BPI), abdominal cramps (AC), decreased appetite (DA), irregular heartbeat (IH), trouble sleeping, abdominal pain, tired and heavy, stomach upset, vomiting, trouble breathing, diarrhea, heartburn, changes in taste, sore mouth, muscle pain, nausea, fever, drowsiness, swelling, chills, seizures, dizziness, rash, and constipation.

For preparing the dataset, collected COVID medicine chemical three-dimensional conformer listed on PubChem was combined with labels of negative medicine responses of the corresponding COVID drugs obtained from WebMD into a multilabel dataset.

3.1.1 | Negative medicine response

The medicine responds extracellularly as per the chemical reactions. Sometimes medicine responses become adverse due to some toxic chemical reactions. Negative medicine reactions are a prominent human health issue caused by the toxic chemical reactions of medicine during the use of medicine to treat diseases. Negative medicine responses are undesirable and unanticipated effects of medicine [8, 34], which are collected from WebMD [33]. This collected information contains data on the market availability of medicine and any observed negative medicine responses. Each medicine has a unique ID, with 17 medicines and 29 negative medicine responses in the collected information.

Several medicine side effects occur in the human body. These side effects appear due to the chemical reactions of medicine. Due to the chemical reactions of the medicine, most of the time, negative medicine reactions occur in the patient body. These negative medicine reactions are associated with chemical conformers, so analyzing chemical conformers is an integral part of drug development. The list of negative medicine reactions and chemical conformers is shown in Table 1.
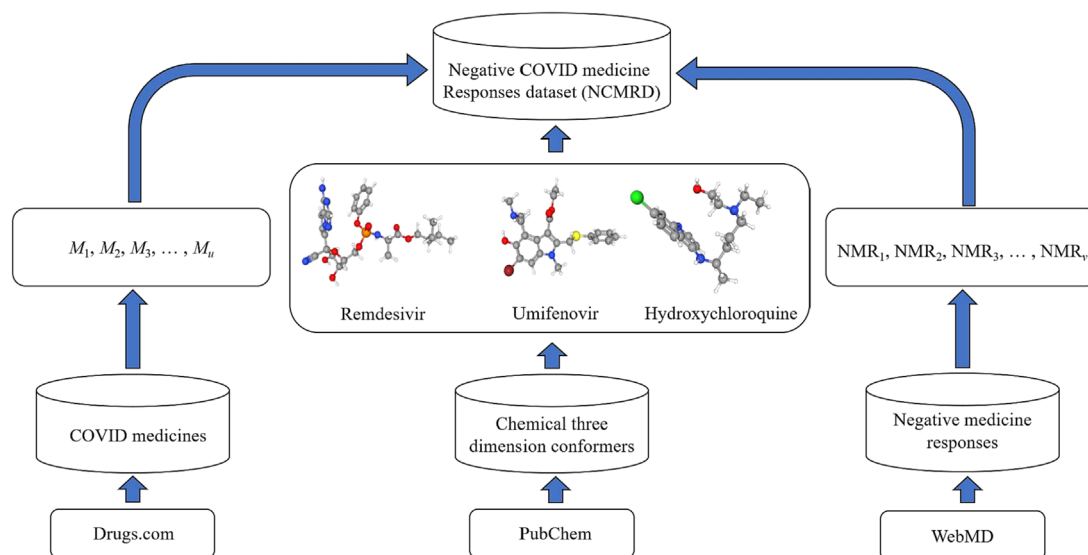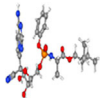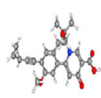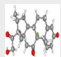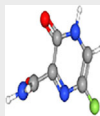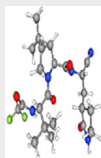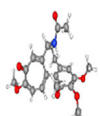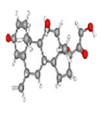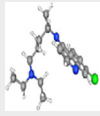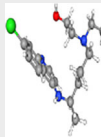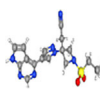

FIGURE 1 Development procedure of Negative COronaVIrus Disease (COVID) Medicine Responses Dataset (NCMRD)

TABLE 1 Medicine and their negative reactions corresponding to chemical three-dimensional (3D) conformer.

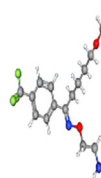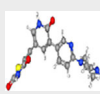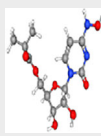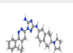| Medicine	Conformer	NMR	Medicine	Conformer	NMR
Remdesivir		Sweating, LFTA, BPI, IH, vomiting, trouble breathing, nausea, fever, swelling, chills, seizures, dizziness, rash, sweating.	Zyesami		Headache, DA, trouble sleeping, vomiting, diarrhea, drowsiness, dizziness
Dexame-thasone		Headache, IH, trouble sleeping, stomach upset, vomiting, trouble breathing, heartburn, nausea, swelling, seizures, dizziness, rash	Peginterferon Lambda		Headache, LFTA, DA, trouble sleeping, tired and heavy, vomiting, diarrhea, nausea, fever, swelling, chills, dizziness, rash
Hydroxy-chloroquine		Sweating, abdominal pain, headache, nausea, vomiting, diarrhea, dizziness, rash.	Umifenovir		Diarrhea, nausea, rash
Favipiravir		Asthma attack, headache, stomach upset, trouble breathing, heartburn, muscle pain, nausea, fever, drowsiness, swelling, dizziness, constipation.	PF-07321332		Vomiting, diarrhea, changes in taste, nausea
Colchicine		Headache, abdominal cramps, abdominal pain, vomiting, diarrhea, nausea	Methyl- prednisolone		Headache, DA, trouble sleeping, vomiting, sweating, heartburn, nausea, dizziness
Chloroquine phosphate		Headache, abdominal cramps, abdominal pain, vomiting, diarrhea, nausea	Hydroxy-chloroquine sulfate		Sweating, headache, DA, trouble sleeping, vomiting, diarrhea, nausea, dizziness
Baricitinib		DA, tired and heavy, abdominal pain, vomiting, nausea, fever	Fluvoxamine		Sweating, weakness, nausea, DA, trouble sleeping, vomiting, drowsiness, dizziness
Protein kinase inhibitors 1		DA, tired and heavy, vomiting, diarrhea, sore mouth, muscle pain, nausea, swelling	MK-4482		Headache, vomiting, diarrhea, nausea, rash
Bemcentinib		DA, Diarrhea			

Abbreviations: BPI, blood pressure increased; DA, decreased appetite; IH, irregular heartbeat; LFTA, liver function test abnormal; NMR, negative medicine responses.

3.1.2 | Chemical three-dimensional conformer

Chemical feature of medicine plays an essential role in drug development [35]. The three-dimensional chemical conformer of medicine is a vital feature of medicine [36]. These conformers are the best view to represent the chemical structure in the image. In a three-dimensional chemical conformer, the associations of the ball and stick represent a chemical compound (medicine) structure that

shows the atom position and the connections that connect them [37]. Typically, spheres are used to represent the atom, while sticks are used to depict the bonds. It is a visual illustration of the chemical bond that holds atoms in molecules together, where functional groupings, chemical chains, and rings are linked in the three-dimensional chemical conformer. A medicine's physicochemical features, as well as its toxicity, excretion, absorption, distribution, and metabolism features, are also associated with the substructure of the conformer. The PubChem database is being used for scraping the chemical three-dimensional conformer [32].

3.2 | Problem statement

Let medicine $= \{M_1, M_2, M_3, ..., M_u\}$ be the set of medicines, where u denotes the total number of medicines ($u = 17$ in this article). Let NMR $= \{NMR_1, NMR_2, ..., NMR_v\}$ be the set of negative medicine responses (NMR), where v is the total number of negative medicine reactions ($v = 29$). Machines understand every image as a matrix of numbers. This matrix's size is dependent on how many pixels are present in the input image. The pixel values assigned to every pixel indicate that particular pixel's brightness and intended colors. Therefore, pixels are the pixel values or numbers that indicate the brightness or intensity of the pixel. Let IMF_red $= \{IMF_{1,1}, IMF_{1,2}, ..., IMF_{r,r}\}$, IMF_green $= \{IMF_{1,1}, IMF_{1,2}, ..., IMF_{r,r}\}$, and IMF_blue $= \{IMF_{1,1}, IMF_{1,2}, ..., IMF_{r,r}\}$ be used to describe a set of three-dimensional conformer feature for RGB channel where r is the RGB matrix cell value ($r = 256$). A medicine can have more than one negative medicine response. Thus, identifying negative medicine responses belongs to a multilabel prediction activity. Figure 2 illustrates the multiple negative medicine responses presentation, where one defines the presence of a negative medicine response and zero defines the absence of a negative medicine response.

The images in the dataset are first converted to a size of $256 \times 256 \times 3$ ($r \times r \times 3$); initial 256 represents the height, next 256 the width, and 3 represents the number of color channels. An image of size $256 \times 256 \times 3$ is a matrix with three layers (RGB), where each layer contains 256×256 values. The computation of large numeric values could become more complicated when using the image as it is and running it through a CNN. To reduce this, we normalize the data to fall between 0 and 1. Since each matrix value ranges from 0 to 255, that indicates the intensity of that pixel's color. Therefore, dividing all numbers by 255 will change the range from 0 to 1. As a result, the calculations will be simpler and quicker because the numbers will be small.
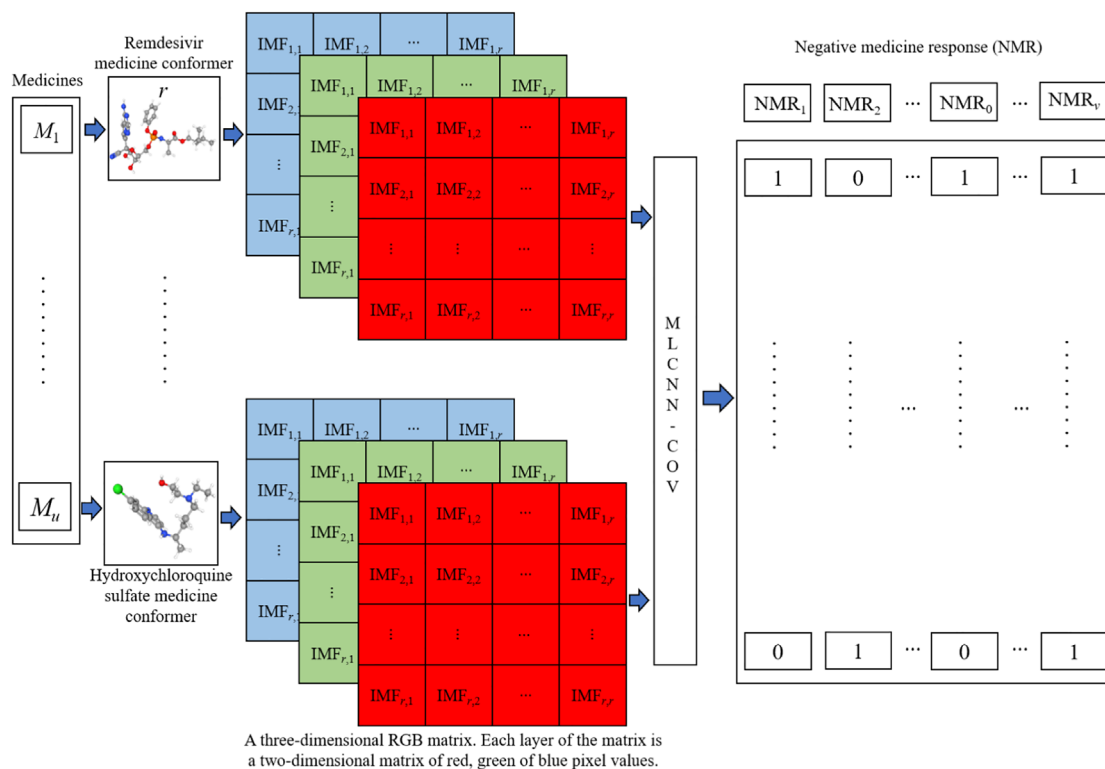

A three-dimensional RGB matrix. Each layer of the matrix is a two-dimensional matrix of red, green of blue pixel values.

FIGURE 2 Illustration of multiple-label negative medicine responses.

A medicine have a three-dimensional chemical conformer, and each medicine has negative responses. So each three-dimensional chemical conformer feature is also related to negative medicine responses.

3.3 | Workflow of proposed methodology

The diagrammatic representation of the workflow of the proposed framework to identify negative COVID medicine responses from the three-dimensional chemical conformer is shown in Figure 3. At first, the three-dimensional chemical conformers are scrapped from PubChem, and negative COVID medicine responses are collected from WebMD. After collecting the three-dimensional conformer, image preprocessing is needed to give as an input feature to MLCNN-COV and pretrained models. Once preprocessing is done, the proposed framework is designed to identify negative medicine responses of COVID medicines. The CNNs model needs a large number of training samples to perform well. So, to improve the model performance, image augmentation has been applied. The performance of the presented model MLCNN-COV classifier is affected by different parameter values of image augmentation techniques. The model performance has been analyzed by setting the distinct values of the parameters of image augmentation and found that the model performed better with the value of shear-range = 0.2, width-shift-range = 0.1, rotation-range = 25, height-shift-range = 0.1, zoom-range = 0.2, fill-mode = "nearest", and horizontal-flip = "True". In the present work, 1 three-dimensional chemical conformer is used to test the model, and 16 new images are generated with the help of image augmentation in each epoch for training (for each conformer, one new augmented image is generated in each epoch). Hence, in 10 epochs, for each conformer, 10 new images are generated for the experiment. In each epoch, the model will get distinct variations of the chemical conformers with the help of ImageDataGenerator class that permits the model to acquire new variations of the chemical conformers. In 10 epochs, 10×16 (160) variations of the images will be generated and fed into the training model. The original chemical conformer of hydroxychloroquine drug has been illustrated in Figure 4 and after applying the image augmentation on the chemical conformer of hydroxychloroquine drug has been shown in Figure 4A–J. The images are generated artificially from the original chemical three-dimensional conformer to improve the performance of the classification models. Furthermore, evaluate the performance of the presented methodology using average hamming-loss (H-L), average accuracy (A), micro average of precision (P), recall (R), and F_1 score, macro average of precision, recall, and F_1 score, and weighted average of precision, recall, and F_1 score and receiver operating characteristic-area under the curve (ROC-AUC) score.

3.4 | Proposed framework

The most used deep learning model for image classification is CNN and transfer-learning models [38, 39]. The two parts of the presented MLCNN-COV framework are presented in Figure 5. The first part was taken for extracting features from the three-dimensional chemical conformer, and the second part classified the three-dimensional chemical conformer into 29 negative COVID medicine responses. Four layers exist for the feature extraction, including the input layer, which contains the three-dimensional chemical conformer for the presented MLCNN-COV framework. Second, a convolutional layer is used where filters are applied to the original chemical three-dimensional conformer. Third, a pooling layer minimizes the computation needed by the MLCNN-COV model, which gradually reduces the input chemical three-dimensional conformer structure spatial dimension. The fourth layer is called the dropout layer. It serves as a mask by removing some neurons' functional processes from the subsequent layer while maintaining the functional processes of other neurons. On the other hand, a fully connected layer is utilized in the second part of the framework to identify negative COVID medicine reactions.
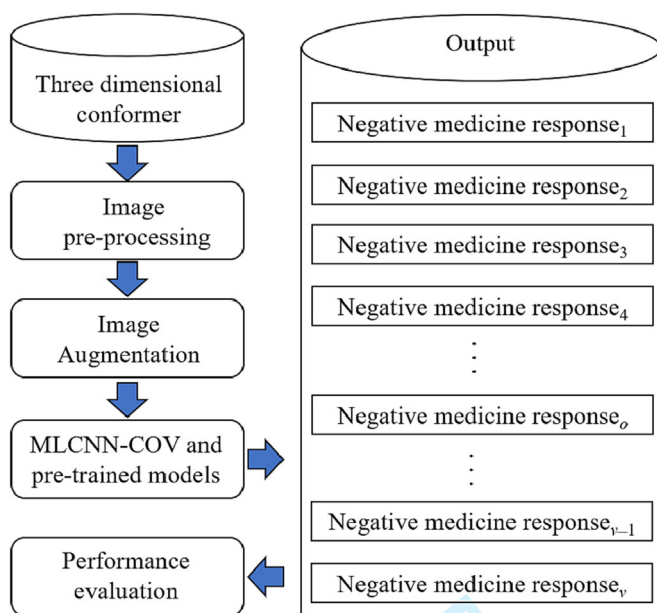
FIGURE 3 Proposed model workflow to identify negative COronaVIrus Disease (COVID) medicine response.

FIGURE 4 The original and new augmented chemical conformer images of hydroxychloroquine drug: (A) original image, (B) augmented image, (C) augmented image, (D) augmented image, (E) augmented image, (F) augmented image, (G) augmented image, (H) augmented image, (I) augmented image, (J) augmented image, (K) augmented image.

(A)   (B)   (C)

(D)   (E)   (F)

(G)   (H)   (I)

(J)   (K)
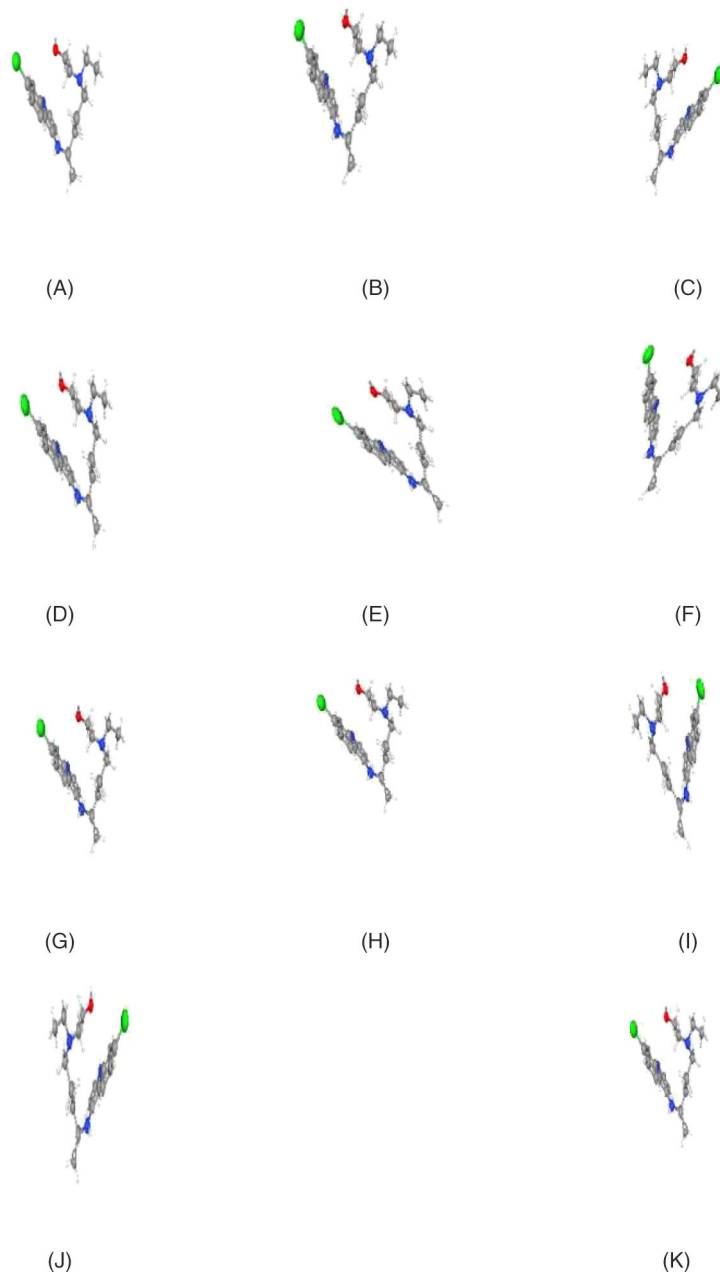
3.4.1 | Feature extraction of the proposed methodology

The procedure of image feature extraction from the chemical conformer has been provided in this section.

A CNN is utilized to extract features from the image of the chemical three-dimensional conformer. The images of chemical three-dimensional conformer are first converted to a size of $256 \times 256 \times 3$, where the three denotes the image's three color channels (R, G, and B). The features of the image of the chemical three-dimensional conformer are extracted utilizing the following stages:

The Convolution2D layer utilizes a set of filters for the input chemical three-dimensional conformer; each filter is a size of a 3×3 matrix of weights. The Convolution2D layer executes a convolution process on the input image of chemical conformer to create a new feature map. Further, an Activation layer applies a nonlinear activation function (in this paper, the ReLU function) to the output of the Convolution2D layer, which allows the model to learn more complicated patterns from the image. The MaxPooling2D layer operates a max pooling operation on the output obtained by the Activation layer. It reduces the feature map's spatial dimensions, which helps decrease the number of parameters in the network
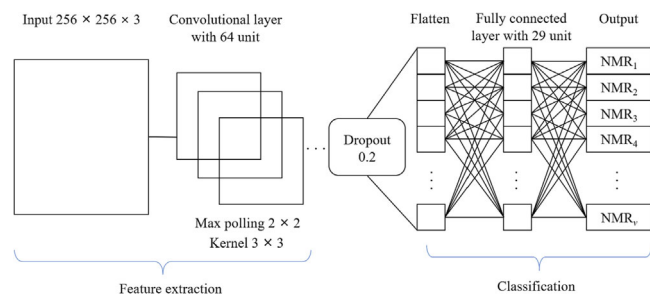
FIGURE 5 Architecture of the presented multilabel convolutional neural network for COVID (MLCNN-COV) model.

and prevents overfitting. The Dropout layer randomly sets a fraction of the output values to zero, which aids in preventing overfitting by minimizing the dependency on any feature. In order to input the data into the next layer, the data must be flattened into a single vector of values which is performed by the Flatten layer. The Dense layer applies a linear transformation to the flattened feature vector, producing a 29 dimensional output vector. The Dense layer represents the final set of image features of the chemical three-dimensional conformer extracted by the network. The Activation layer produces the final output vector of probabilities by applying the sigmoid activation function to the Dense layer's output. The output produced by this layer can be utilized for identifying negative medicine responses by utilizing a threshold value. These features are learned by the model during training and can be used to represent the visual content of the image of a three-dimensional chemical conformer in a compact and useful form.

3.5 | Transfer-learning

Transfer-learning has become an essential part of the modern image classification problem. Transfer-learning models play a crucial role and are being utilized to solve complex tasks in modern drug development research. For identifying negative COVID medicine responses, five multilabel transfer-learning models, namely, Mobile-Netv2, ResNet50, VGG19, DenseNet201, and Inceptionv3, and an MLCNN-COV model are designed with an image augmentation technique.

- MobileNetV2: In order to function well on mobile devices, MobileNetV2 transfer-learning is designed. It is built on an inverted residual architecture so that the residual connections connect the bottleneck layers. Lightweight depthwise convolutions are used in the intermediate expansion layer as a source of nonlinearity to filter features. The MobileNetV2 architecture

includes a 32-filter with an initial fully convolution layer as well as 19 residual bottleneck layers [40, 41].
- DenseNet201: DenseNet is based on the notion that convolutional networks may be trained to be significantly deeper, more precise, and more effective if they have shorter connections between layers that are close to the input and those that are close to the output. The DenseNet-201 transfer-learning model consists of a CNN with 201 layers deep [42].
- ResNet50: Residual Network is abbreviated as ResNet. It is a residual network with 50 layers [43, 44]. Sometimes the performance of DNN starts to decrease when add more layers. This occurs as a result of the vanishing gradient issue. When they are backpropagated through the DNN and repeatedly multiplied, gradients become particularly small and cause the vanishing gradient issue. By employing identity bypass connections that skip more than one layer, ResNet50 is able to address the vanishing gradient issue.
- Inceptionv3: Inceptionv3 is the third version of Google's Inception CNN. Inceptionv3 was created to enable deeper networks while keeping an excessive amount of parameters from being used. Inceptionv3 is a CNN that consists of 48 layers deep [45].
- VGG19: Visual Geometry Group is known as VGG. It has several layers and is a typical deep CNN architecture. The term "deep" describes the amount of layers, with VGG19 having 19 convolutional layers [46, 47]. This transfer-learning model is based on the essential features of CNN. This network has learned rich feature representation for a wide range of the image.

3.6 | Parameter settings

In this section, the MLCNN-COV and multilabel transfer-learning framework parameters have been demonstrated.

Leave-one-out cross-validation is utilized to evaluate the experiment with the help of the Python programming language in Google Colab. Sequential API, Keras, and TensorFlow are employed to construct the presented MLCNN-COV model and transfer-learning framework. Different parameters of the MLCNN-COV model and transfer-learning models have an impact on the performance of the experiment. Hence, the presented framework have been evaluated with distinct parameters. The performance of the proposed framework (MLCNN-COV) with several numbers of convolutional layers is shown in Figure 6. In the first MLCNN-COV model convolutional layers with 16 filters, the second MLCNN-COV model convolutional layers with 32 filters and the third MLCNN-COV model convolutional layers with 64 filters
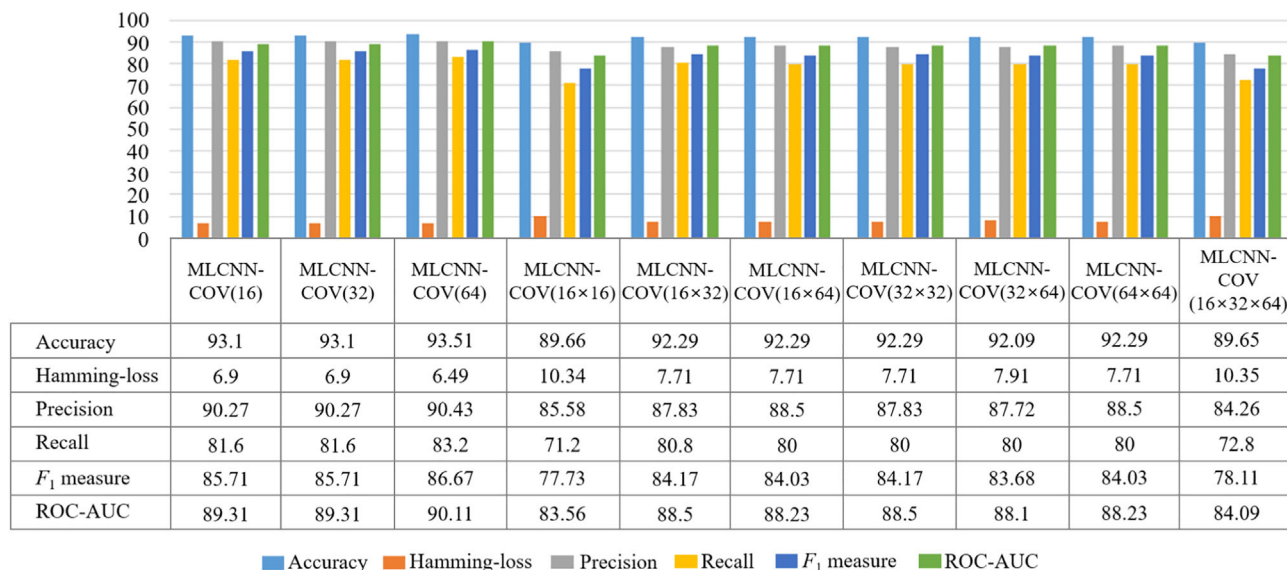
	MLCNN-COV(16)	MLCNN-COV(32)	MLCNN-COV(64)	MLCNN-COV(16×16)	MLCNN-COV(16×32)	MLCNN-COV(16×64)	MLCNN-COV(32×32)	MLCNN-COV(32×64)	MLCNN-COV(64×64)	MLCNN-COV(16×32×64)
Accuracy	93.1	93.1	93.51	89.66	92.29	92.29	92.29	92.09	92.29	89.65
Hamming-loss	6.9	6.9	6.49	10.34	7.71	7.71	7.71	7.91	7.71	10.35
Precision	90.27	90.27	90.43	85.58	87.83	88.5	87.83	87.72	88.5	84.26
Recall	81.6	81.6	83.2	71.2	80.8	80	80	80	80	72.8
F_1 measure	85.71	85.71	86.67	77.73	84.17	84.03	84.17	83.68	84.03	78.11
ROC-AUC	89.31	89.31	90.11	83.56	88.5	88.23	88.5	88.1	88.23	84.09

FIGURE 6 Different parameters performance of multilabel convolutional neural network for COVID (MLCNN-COV) model to identify negative COronaVIrus Disease (COVID) medicine responses.

are used, respectively, and so on with their combination and found that the convolutional layer with 64 filters with dropout rate 0.2 performs well. For all the convolutional layers, Relu activation function is employed. In order to carry out the experiment, the MLCNN-COV framework utilized RGB channel and resized the chemical three-dimensional conformer structure to 256×256 pixels with Max Pooling with 2×2 window size and 3×3 kernel sizes for all convolutional layers. Different dropout rates have been imported to evaluate how well the framework works. Furthermore, it is noticed that the performance of the MLCNN-COV framework is not enhanced as the dropout rate increases to 0.2. To build the MLCNN-COV framework, binary cross entropy is set for the loss function, and the optimizer is set to adam. The epoch number is set to 10 with the help of a learning rate of 0.0001, and the sigmoid activation function is employed in the fully connected layer for output. The COVID medicines may have multiple negative medicine responses, which is referred to as the multilabel classification activity. As a result, the model's final layer is constructed using 29 neurons, which is the same as the total number of labels with a threshold value of 0.5.

Sequential API, Keras, and TensorFlow (tf) are employed to construct the transfer-learning models: for MobileNetV2 tf.keras.applications.MobileNetV2, for DenseNet201 tf.keras.applications.DenseNet201, for ResNet50 tf.keras.applications.ResNet50, for Inceptionv3 tf.keras.applications.inception_v3.InceptionV3, for VGG19 tf.keras.applications. VGG19 have been imported from TensorFlow-Keras to implement transfer-learning models.

For all the transfer-learning models, the input shape is set to (256, 256, 3), and weights are set to "imagenet". The transfer-learning models have also been tested with distinct parameters and found that with a dropout rate of 0.2 and setting Global AveragePooling2D achieved a good result. To build the transfer-learning models, binary cross entropy is set for the loss function, and the optimizer is set to adam. The epoch number is set to 10 with the help of a learning rate of 0.0001, and the sigmoid activation function is employed in the output layer for output. The COVID medicines can have more than one adverse medicine response, so the problem belongs to multilabel classification activity. As a result, the model's final layer is constructed using 29 neurons, which is the same as the total number of labels with a threshold value of 0.5.

4 | EXPERIMENTAL RESULTS AND DISCUSSION

This section provides the performance measurement details and experimental results of the presented framework to identify negative COVID medicine responses from the three-dimensional chemical conformer.

4.1 | Performance measurement

This section presents the multilabel algorithms performance metric to analyze how well they identified negative responses of COVID medicine. The example-based

strategy has been used to evaluate the performances [48, 49]. Let us assume AL as a set of Actual Labels (AL) that are present in an example s_i and TL(s_i) be the set of labels that the MLCNN-COV and transfer-learning computational methods predict.

$$\text{Accuracy} = \frac{1}{N} \sum_{i=1}^{N} \frac{|\text{TL}(s_i) \cap \text{AL}_i|}{|\text{TL}(s_i) \cup \text{AL}_i|}, \tag{1}$$

$$\text{Hamming-loss} = \frac{1}{N} \sum_{i=1}^{N} \frac{1}{c} |\text{TL}(s_i) \Delta \text{AL}_i|, \tag{2}$$

$$\text{Precision} = \frac{1}{N} \sum_{i=1}^{N} \frac{|\text{TL}(s_i) \cap \text{AL}_i|}{|\text{AL}_i|}, \tag{3}$$

$$\text{Recall} = \frac{1}{N} \sum_{i=1}^{N} \frac{|\text{TL}(s_i) \cap \text{AL}_i|}{|\text{TL}(s_i)|}, \tag{4}$$

$$F_1 = \frac{1}{N} \sum_{i=1}^{N} \frac{2|\text{TL}(s_i) \cap \text{AL}_i|}{|\text{TL}(s_i)| + |\text{AL}_i|}. \tag{5}$$

In the equations above, N stands for the total count of instances, c for the number of possible labels, and Δ for the symmetry difference between the predicted label and actual label sets.

ROC-AUC is one of the most crucial probabilistic score evaluation criteria for analyzing the effectiveness of multilabel models. It shows how well the computational transfer-learning models can classify the distinct classes at various threshold levels and serves as a degree or indicator of class separability.

4.2 | Results

This section provides the performance study of the presented MLCNN-COV and its comparative study with Inceptionv3, MobileNetv2, VGG19, DenseNet201, and ResNet50 transfer-learning models.

From Table 2, it can be observed that the MLCNN-COV classifier outperformed the transfer-learning model's performance. MLCNN-COV classifiers achieved the highest average accuracy score of 93.51%, and it can identify individual adverse reactions of COVID medicines, with accuracy ranging from 82.35% to 100%. It can be observed from Table 2 that for the MLCNN-COV classifier model, negative medicine reactions include AC, asthma attack, changes in taste, constipation, heartburn, muscle pain, sore mouth, stomach upset, and tired and heavy that are expressed fully (100%). In contrast, most

other negative medicine reactions are expressed in an accuracy range of 82.35% to 94.12%. After applying the image augmentation technique to train the MLCNN-COV framework effectively, it can be observed from Table 3 that the MLCNN-COV classifier performs well and achieved the highest average accuracy score of 97.16%. The MLCNN-COV classifier with image augmentation was applied on the image of the three-dimensional chemical conformer; 17 negative COVID medicine responses (abdominal cramps, asthma attack, changes in taste, constipation, heartburn, muscle pain, sore mouth, stomach upset, tired and heavy, BPI, chills, fever, IH, liver function test abnormal, seizures, swelling, and trouble breathing) among the 29 negative medicine reactions has achieved the highest 100% accuracy for each negative medicine reactions. In contrast, the remaining negative medicine reactions (abdominal pain, DA, diarrhea, dizziness, drowsiness, headache, nausea, rash, sweating, trouble sleeping, weakness, and vomiting) achieved accuracy in the range of 88.24% to 94.12%.

On the other hand, among the transfer-learning models, the Inceptionv3 and MobileNetv2 classifiers performed well. It can be observed from Table 2 that the Inceptionv3 and MobileNetv2 classifier models achieved individual negative medicine reactions accuracy in a range of 58.82% to 100% and achieved an average accuracy score of 82.76%. On evaluating the model performance with image augmentation across each adverse medicine reaction, it has been observed that the models performance has improved, which can be observed from Table 3. The Inceptionv3 classifier model achieved an average accuracy score of 92.09% and individual negative medicine reactions accuracy in the range of 64.71% to 100%. The Inceptionv3 classifier model expressed fully for some adverse medicine reactions (abdominal cramps, asthma attack, changes in taste, constipation, heartburn, and tired and heavy) and achieved 100% accuracy. After applying the image augmentation, the MobileNetv2 classifier model performance has also improved and achieved an average accuracy score of 86.64% and accuracy for individual negative medicine reactions in the range of 70.59% to 100%. The MobileNetv2 classifier identifies three adverse medicine reactions (asthma attack, constipation, and dizziness) 100% accurately, which can be observed from Table 3.

It can be noticed from Table 2 that the VGG19 classifier model has achieved accuracy in the range of 35.29% to 94.12% for each adverse medicine reaction and a 79.31% average accuracy score. On analysis of individual negative medicine reaction-wise after applying image augmentation, VGG19 classifier model accuracy was achieved in the range of 58.82% to 94.12%, and the

TABLE 2 Accuracy score of the MLCNN-COV and transfer-learning models to identify individual negative medicine responses from three-dimensional chemical conformer.

Class	MLCNN-COV	Inceptionv3	MobileNetv2	VGG19	DenseNet201	ResNet50
AC	100	88.24	76.47	76.47	82.35	88.24
Abdominal pain	94.12	70.59	76.47	76.47	70.59	64.71
Asthma attack	100	94.12	100	88.24	94.12	94.12
BPI	94.12	94.12	94.12	94.12	94.12	94.12
Changes in taste	100	94.12	94.12	88.24	94.12	94.12
Chills	94.12	88.24	94.12	88.24	88.24	88.24
Constipation	100	94.12	94.12	94.12	94.12	94.12
DA	88.24	76.47	58.82	52.94	64.71	17.65
Diarrhea	88.24	58.82	76.47	64.71	76.47	64.71
Dizziness	88.24	58.82	58.82	35.29	58.82	52.94
Drowsiness	94.12	82.35	70.59	82.35	76.47	76.47
Fever	94.12	82.35	58.82	76.47	76.47	76.47
Headache	82.35	76.47	64.71	58.82	64.71	58.82
Heartburn	100	88.24	82.35	82.35	76.47	82.35
IH	88.24	88.24	88.24	88.24	88.24	82.35
LFTA	94.12	94.12	94.12	94.12	88.24	94.12
Muscle pain	100	82.35	94.12	88.24	64.71	70.59
Nausea	94.12	82.35	82.35	88.24	88.24	88.24
Rash	82.35	64.71	64.71	64.71	64.71	64.71
Seizures	88.24	88.24	88.24	88.24	88.24	88.24
Sore mouth	100	88.24	94.12	94.12	88.24	76.47
Stomach upset	100	88.24	94.12	82.35	88.24	88.24
Sweating	82.35	76.47	76.47	76.47	76.47	76.47
Swelling	94.12	70.59	88.24	70.59	94.12	58.82
Tired and heavy	100	82.35	82.35	76.47	82.35	82.35
Trouble breathing	88.24	100	94.12	88.24	88.24	82.35
Trouble sleeping	94.12	82.35	82.35	70.59	76.47	70.59
Vomiting	94.12	82.35	82.35	82.35	82.35	82.35
Weakness	94.12	82.35	94.12	88.24	94.12	94.12
Average accuracy	**93.51**	**82.76**	**82.76**	**79.31**	**81.54**	**77.49**

Abbreviations: AC, abdominal cramps; MLCNN-COV, multilabel convolutional neural network for COVID.

average accuracy achieved by the model is 82.76%, which can be observed from Table 3.

For each negative medicine reaction, the performance of the DenseNet201 classifier model has been observed from Table 2. It achieved accuracy on each negative medicine response in the range of 58.82% to 94.12% and average accuracy of 81.54%. In the study of each negative medicine reaction-wise after applying image augmentation technique, accuracy is achieved in the range of 64.71% to 100%, and the average accuracy achieved by the DenseNet201 model is 88.03%. The DenseNet201

classifier model expressed fully for Constipation adverse medicine reactions and achieved 100% accuracy, which can be observed from Table 3.

It can be observed from Table 2 that the ResNet50 classifier model achieved individual negative medicine reactions accuracy in a range of 17.65% to 94.12% and got an average accuracy score of 77.49%. Further, Table 3 shows that the individual adverse medicine reactions accuracy range is improved in a range of 47.06% to 94.12% after applying the image augmentation technique and achieved an average accuracy score of 81.34%.

TABLE 3 Accuracy score of the MLCNN-COV and transfer-learning models after applying image augmentation technique to identify individual negative medicine responses from three-dimensional chemical conformer.

Class	MLCNN-COV+IA	Inceptionv3+IA	MobileNetv2+IA	VGG19+IA	DenseNet201+IA	ResNet50+IA
AC	100	100	84.24	88.24	88.24	88.24
Abdominal pain	94.12	94.12	70.59	76.47	76.47	76.47
Asthma attack	100	100	100	94.12	94.12	94.12
BPI	100	94.12	94.12	94.12	94.12	94.12
Changes in taste	100	100	94.12	94.12	94.12	94.12
Chills	100	94.12	88.24	88.24	88.24	88.24
Constipation	100	100	100	94.12	100	94.12
DA	88.24	88.24	76.47	76.47	82.35	58.82
Diarrhea	94.12	94.12	76.47	64.71	82.35	64.71
Dizziness	94.12	88.24	100	58.82	94.12	47.06
Drowsiness	94.12	94.12	88.24	82.35	82.35	82.35
Fever	100	94.12	94.12	76.47	88.24	76.47
Headache	94.12	88.24	94.12	70.59	94.12	58.82
Heartburn	100	100	88.24	82.35	82.35	82.35
IH	100	88.24	88.24	88.24	88.24	88.24
LFTA	100	94.12	94.12	94.12	94.12	94.12
Muscle pain	100	94.12	94.12	88.24	88.24	88.24
Nausea	94.12	88.24	88.24	88.24	88.24	88.24
Rash	94.12	64.71	70.59	64.71	64.71	64.71
Seizures	100	88.24	88.24	88.24	88.24	88.24
Sore mouth	100	94.12	94.12	94.12	94.12	94.12
Stomach upset	100	94.12	94.12	88.24	88.24	88.24
Sweating	88.24	76.47	76.47	76.47	76.47	76.47
Swelling	100	88.24	82.35	70.59	94.12	70.59
Tired and heavy	100	100	88.24	82.35	82.35	82.35
Trouble breathing	100	88.24	88.24	88.24	88.24	88.24
Trouble sleeping	94.12	94.12	88.24	70.59	94.12	70.59
Vomiting	94.12	94.12	88.24	82.35	88.24	82.35
Weakness	94.12	94.12	94.12	94.12	94.12	94.12
Average accuracy	**97.16**	**92.09**	**86.64**	**82.76**	**88.03**	**81.34**

Abbreviations: AC, abdominal cramps; BPI, blood pressure increased; DA, decreased appetite; IA, image augmentation; IH, irregular heartbeat; LFTA, liver function test abnormal; MLCNN-COV, multilabel convolutional neural network for COVID.

The performance of the presented MLCNN-COV model has been evaluated and compared with Inceptionv3, MobileNetv2, VGG19, DenseNet201, and ResNet50. It can be observed from Table 4 that the MLCNN-COV model performed the best and achieved the highest micro average precision (MiAP) score of 90.43%, macro average precision (MaAP) score of 74.63%, weighted average precision (WAP) score of 84.64%, micro

TABLE 4 Results of the MLCNN-COV and transfer-learning models on the chemical three-dimensional conformer structure to identify negative COVID medicine responses.

Model	H-L	MiAP	MaAP	WAP	MiAR	MaAR	WAR	MiAF1	MaAF1	WAF1	ROC
MLCNN-COV	6.49	90.43	74.63	84.64	83.20	70.88	83.20	86.67	71.57	83.14	90.11
MLCNN-COV+IA	2.84	93.70	93.12	93.40	95.20	92.99	95.20	94.44	92.75	93.92	96.51
Inceptionv3	17.24	71.74	33.32	57.50	52.80	25.71	52.80	60.83	26.99	52.44	72.87
Inceptionv3+IA	7.91	93.00	68.73	82.07	74.40	58.31	74.40	82.67	61.82	76.73	86.25
MobileNetv2	17.24	67.86	41.86	57.80	60.80	37.10	60.80	64.14	37.24	57.17	75.51
MobileNetv2+IA	11.36	89.66	56.86	76.44	62.40	39.02	62.40	73.58	43.55	64.93	79.98
VGG19	20.69	63.53	11.52	33.09	43.20	15.33	43.20	51.43	13.06	37.24	67.39
VGG19+IA	17.24	75.00	15.00	40.67	48.00	17.00	48.0	58.00	16.31	43.49	71.28
DenseNet201	18.46	67.00	30.51	55.99	53.60	27.82	53.60	59.56	26.23	51.08	72.32
DenseNet201+IA	11.97	90.24	34.45	63.00	59.20	30.00	59.20	71.50	31.38	59.92	78.51
ResNet50	22.51	56.03	19.40	38.00	52.00	31.30	52.00	53.94	23.53	43.51	69.07
ResNet50+IA	18.66	70.37	15.31	40.21	45.60	15.52	45.60	55.34	14.35	39.74	69.54

Abbreviations: H-L, hamming-loss; MaAF1, macro average F_1; MaAP, macro average precision; MaAR, macro average recall; MiAF1, micro average F_1; MiAP, micro average precision; MiAR, micro average recall; WAF1, weighted average F_1; WAP, weighted average precision; WAR, weighted average recall.

average recall (MiAR) value of 83.20%, macro average recall (MaAR) value of 70.88%, weighted average recall (WAR) value of 83.20%, micro average F_1 (MiAF1) measure of 86.67%, macro average F_1 (MaAF1) measure of 71.57%, weighted average F_1 (WAF1) measure of 83.14%, and average ROC score of 90.11%, and the lowest average H-L of 6.49%. After image augmentation, it can be noticed that the MLCNN-COV framework with image augmentation achieved the highest MiAR, MaAR, WAR, micro average F1, macro average F1, weighted average F1, MiAP, MaAP, and WAP, as well as the lowest average H-L on three-dimensional chemical conformer, which can be observed from Table 4. On the other hand, without image augmentation technique among the transfer-learning models, the Inceptionv3 and MobileNetv2 classifiers model achieved the lowest H-L of 17.24%. For MiAP, the Inceptionv3 model achieved the highest score of 71.74%. On the other hand, the MobileNetv2 model achieved the highest MaAP score of 41.86%, WAP of 57.80%, MiAR value of 60.80%, MaAR score of 37.10%, WAR value of 60.80%, MiAF1 measure of 64.14%, MaAF1 measure of 37.24%, WAF1 measure of 57.17%, and average ROC value of 75.51%. After applying the image augmentation technique, the Inceptionv3 classifier models performed the best among the transfer-learning model, which can be observed from Table 4.

The ROC-AUC score of MLCNN-COV and the transfer-learning models are shown in Table 4. It can be observed from Table 4 that the MLCNN-COV model achieved the highest ROC-AUC score of 90.11%

compared with the transfer-learning model's performance. Also, after applying the image augmentation technique to train the framework effectively, it can be observed from Table 4 that the MLCNN-COV classifier achieved the highest ROC-AUC score of 96.51% compared with other transfer-learning classifiers models. On the performance of the classifier-wise ROC-AUC, the six classifier models have been ranked as MLCNN-COV > MobileNetv2 > Inceptionv3 > DenseNet201 > ResNet50 > VGG19 with respect to their potential to predict negative COVID medicine reactions. After applying the image augmentation technique, ROC-AUC score of MLCNN-COV and the transfer-learning models are shown in Table 4. Regarding the classifier's ROC-AUC performance with image augmentation, the six models have ranked as MLCNN-COV > Inceptionv3 > MobileNetv2 > DenseNet201 > VGG19 > ResNet50 to identify negative COVID medicine reactions.

The transfer-learning models have misclassified more negative medicine reactions than the MLCNN-COV model. Based on the average H-L of each classifier, the models are ranked as MLCNN-COV > Inceptionv3 > MobileNetv2 > DenseNet201 > VGG19 > ResNet50 to identify adverse COVID medicine reactions. Image augmentation has played a vital role in training the model effectively across distinct negative medicine reactions. It shows that the average H-L of MLCNN-COV and transfer-learning models has decreased after images are generated artificially from the original chemical three-dimensional conformer to improve the performance of the classification models.

5 | CONCLUSIONS

Medicines typically get approval based on the clinical studies and trial phases, which generally check the adverse negative responses of medicine on a tissue or cell. Therefore, it is common that several medications have been taken off from the market in recent years due to their negative responses. Identifying adverse medicine reactions is costly, tedious, takes billions of capital and human resources, and needs several clinical trial phases with lots of chemical wastage. So, computational models for a medicine's life cycle are especially needed to accurately identify and analyze negative responses. This study contributes to the solution of this issue by designing a multilabel MLCNN-COV and transfer-learning methodology with an image augmentation technique that utilizes an image of the chemical three-dimensional conformer structure for negative COVID medicine reactions detection. The image of the chemical three-dimensional conformer is used as input, where image features are represented using an RGB color channel to predict negative COVID medicine reactions. Further, the image features are extracted by employing the Convolution2D layer and MaxPooling2D layer. Five transfer-learning methods, including Mobile-Netv2, ResNet50, VGG19, DenseNet201, and Inceptionv3, were utilized to examine the experiments, and it found that MobileNetV2 performed well compared with other transfer-learning methods. In contrast, the MLCNN-COV model performed best among the models under consideration. The findings imply that chemical three-dimensional conformer structure data help identify negative COVID medicine responses. The suggested methodology can also be used in COVID medication development to examine negative COVID medicine responses.

CONFLICT OF INTEREST STATEMENT
The authors declare that there are no conflicts of interest.

DATA AVAILABILITY STATEMENT
The extracted datasets are available with authors; on request, these datasets will be made available by the author.

ORCID
Pranab Das https://orcid.org/0000-0002-3757-4118
Dilwar Hussain Mazumder https://orcid.org/0000-0002-6316-2977

REFERENCES

1. C. S. B. Chia, W. Xu, and P. Shuyi Ng, *A patent review on SARS Coronavirus main protease (3CLpro) inhibitors*, Chem. Med. Chem. **17** (2022), no. 1, e202100576.

2. I. A. Seliem, A. S. Girgis, Y. Moatasim, A. Kandeil, A. Mostafa, M. A. Ali, M. S. Bekheit, and S. S. Panda, *New pyrazine conjugates: synthesis, computational studies, and antiviral properties against SARS-CoV-2*, Chem. Med. Chem. **16** (2021), no. 22, 3418–3427.

3. A. K. Ghosh, M. Brindisi, D. Shahabi, M. E. Chapman, and A. D. Mesecar, *Drug development and medicinal chemistry efforts toward SARS-Coronavirus and Covid-19 therapeutics*, Chem. Med. Chem. **15** (2020), no. 11, 907–932.

4. S. Gorai, V. Junghare, K. Kundu, S. Gharui, M. Kumar, B. S. Patro, S. K. Nayak, S. Hazra, and S. Mula, *Synthesis of dihydro-benzofuro [3, 2-b] chromenes as potential 3CLpro inhibitors of SARS-CoV-2: a molecular docking and molecular dynamics study*, Chem. Med. Chem. **17** (2022), no. 8, e202100782.

5. J. Li, Z. Zhang, R. Amini, and Y. Li, One solution for all: searching for universal aptamers for constantly mutating spike proteins of SARS-CoV-2, 2022. ChemMedChem.

6. M. J. C. Long and Y. Aye, *Science's response to Covid-19*, Chem. Med. Chem. **16** (2021), no. 15, 2288–2314.

7. S. Q. Pantaleão, P. O. Fernandes, J. E. Gonçalves, V. G. Maltarollo, and K. M. Honorio, *Recent advances in the prediction of pharmacokinetics properties in drug design studies: a review*, Chem. Med. Chem. **17** (2022), no. 1, e202100542.

8. P. Das, Yogita, and V. Pal, *Integrative analysis of chemical properties and functions of drugs for adverse drug reaction prediction based on multi-label deep neural network*, J. Integrative Bioinform. **19** (2022) no. 3. https://doi.org/10.1515/jib-2022-0007

9. P. Das, J. W. Sangma, and V. Pal, *Predicting adverse drug reactions from drug functions by binary relevance multi-label classification and MLSMOTE*, (15th International Conference on Practical Applications of Computational Biology & Bioinformatics), 2021, pp. 165–173.

10. O. C. Uner, R. G. Cinbis, O. Tastan, and A. E. Cicek, *Deepside: a deep learning framework for drug side effect prediction*, Biorxiv **2019** (2019), 843029.

11. C.-S. Wang, P.-J. Lin, C.-L. Cheng, S.-H. Tai, Y.-H. K. Yang, and J.-H. Chiang, *Detecting potential adverse drug reactions using a deep neural network model*, J. Med. Internet Res. **21** (2019), no. 2, e11016.

12. R. Ietswaart, S. Arat, A. X. Chen, S. Farahmand, B. Kim, W. DuMouchel, D. Armstrong, A. Fekete, J. J. Sutherland, and L. Urban, *Machine learning guided association of adverse drug reactions with in vitro target-based pharmacology*, EBioMedicine **57** (2020), 102837.

13. S. S. Güneş, C. Yeşil, E. E. Gurdal, E. E. Korkmaz, M. Yarım, A. Aydın, and H. Sipahi, *Primum non nocere: in silico prediction of adverse drug reactions of antidepressant drugs*, Comput. Toxicol. **18** (2021), 100165.

14. S. Shankar, I. Bhandari, D. T. Okou, G. Srinivasa, and P. Athri, *Predicting adverse drug reactions of two-drug combinations using structural and transcriptomic drug representations to train an artificial neural network*, Chem. Biol. Drug Design **97** (2021), no. 3, 665–673.

15. M. M. Hatmal, M. A. I. Al-Hatamleh, A. N. Olaimat, M. Hatmal, D. M. Alhaj-Qasem, T. M. Olaimat, and R. Mohamud, *Side effects and perceptions following Covid-19 vaccination in Jordan: a randomized, cross-sectional study implementing machine learning for predicting severity of side effects*, Vaccines **9** (2021), no. 6, 556.

16. D. N. Swathi, *Predicting drug side-effects from open source health forums using supervised classifier approach*, (5th International Conference on Communication and Electronics Systems, Coimbatore, India), 2020, pp. 796–800.

17. S. Jamal, W. Ali, P. Nagpal, S. Grover, and A. Grover, *Computational models for the prediction of adverse cardiovascular drug reactions*, J. Trans. Med. **17** (2019), no. 1, 1–13.

18. S. Jamal, S. Goyal, A. Shanker, and A. Grover, *Predicting neurological adverse drug reactions based on biological, chemical and phenotypic properties of drugs using machine learning models*, Sci. Rep. **7** (2017), no. 1, 1–12.

19. Y. Pouliot, A. P. Chiang, and A. J. Butte, *Predicting adverse drug reactions using publicly available PubChem BioAssay data*, Clin. Pharmacol. Therapeut. **90** (2011), no. 1, 90–99.

20. Y. Liu, P. LePendu, S. Iyer, and N. H. Shah, *Using temporal patterns in medical records to discern adverse drug events from indications*, AMIA Summits on Trans. Sci. Proc. **2012** (2012), 47.

21. M. J. Jahid and J. Ruan, *An ensemble approach for drug side effect prediction*, (IEEE International Conference on Bioinformatics and Biomedicine, Shanghai, China), 2013, pp. 440–445.

22. K. Jiang and Y. Zheng, *Mining twitter data for potential drug effects*, (9th International Conference on Advanced Data Mining and Applications, Hangzhou, China), 2013, pp. 434–443.

23. L.-C. Huang, X. Wu, and J. Y. Chen, *Predicting adverse drug reaction profiles by integrating protein interaction networks with drug structures*, Proteomics **13** (2013), no. 2, 313–324.

24. M. X. LaBute, X. Zhang, J. Lenderman, B. J. Bennion, S. E. Wong, and F. C. Lightstone, *Adverse drug reaction prediction using scores produced by large-scale drug-protein target docking on high-performance computing machines*, PloS One **9** (2014), no. 9, e106298.

25. W. Zhang, F. Liu, L. Luo, and J. Zhang, *Predicting drug side effects by multi-label learning and ensemble learning*, BMC Bioinf. **16** (2015), no. 1, 1–11.

26. S.-Y. Niu, M.-Y. Xin, J. Luo, M.-Y. Liu, and Z.-R. Jiang, *DSEP: a tool implementing novel method to predict side effects of drugs*, J. Comput. Biol. **22** (2015), no. 12, 1108–1117.

27. P. Hu, Z.-H. You, T. He, S. Li, S. Gu, and K. C. C. Chan, *Learning latent patterns in molecular data for explainable drug side effects prediction*, (IEEE International Conference on Bioinformatics and Biomedicine, Madrid, Spain), 2018, pp. 1163–1169.

28. F. Odeh and A. Taweel, *A deep learning approach to extracting adverse drug reactions*, (IEEE/ACS 16th International Conference on Computer Systems and Applications, Abu Dhabi, United Arab Emirates), 2019, pp. 1–6.

29. J. Wang, Y. Deng, L. Shu, and L. Deng, *Machine learning-based methods and novel data models to predict adverse drug reaction*, (IEEE International Conference on Bioinformatics and Biomedicine, Seoul, Rep. of Korea), 2020, pp. 1226–1230.

30. D. A. Nguyen, C. H. Nguyen, and H. Mamitsuka, *A survey on adverse drug reaction studies: data, tasks and machine learning methods*, Brief. Bioinf. **22** (2021), no. 1, 164–177.

31. P. Das and D. H. Mazumder, *An extensive survey on the use of supervised machine learning techniques in the past two decades for prediction of drug side effects*, Artif. Intell. Rev. **2023** (2023), 1–28.

32. S. Kim, J. Chen, T. Cheng, A. Gindulyte, J. He, S. He, Q. Li, B. A. Shoemaker, P. A. Thiessen, and B. Yu, *PubChem 2019 update: improved access to chemical data*, Nucleic Acids Res. **47** (2019), no. D1, D1102–D1109.

33. SEED BLACK, *Uses, side effects, interactions and warnings—WebMD*, WebMD.

34. P. Das and D. H. Mazumder, *Predicting drug functions from adverse drug reactions by multi-label deep neural network*, Multimodal AI in healthcare, Springer, 2023, pp. 215–226.

35. P. Das, Y. Thakran, S. R. N. Anal, V. Pal, and A. Yadav, *BRMCF: binary relevance and MLSMOTE based computational framework to predict drug functions from chemical and biological properties of drugs*, IEEE/ACM Trans. Comput. Biology Bioinform. (2022). https://doi.org/10.1109/TCBB.2022.3215645

36. E. E. Bolton, J. Chen, S. Kim, L. Han, S. He, W. Shi, V. Simonyan, Y. Sun, P. A. Thiessen, and J. Wang, *PubChem3D: a new resource for scientists*, J. cheminf. **3** (2011), no. 1, 1–15.

37. Ball-and-stick model, Wikimedia Foundation, 2022. https://en.wikipedia.org/wiki/Ball-and-stick_model, Accessed on 21.11.2022.

38. Q. Dong, R. Ye, and G. Li, *Crime amount prediction based on 2D convolution and long short-term memory neural network*, ETRI J. **44** (2022), no. 2, 208–219.

39. H. Kim, *A low-cost compensated approximate multiplier for Bfloat16 data processing on convolutional neural network inference*, ETRI J. **43** (2021), no. 4, 684–693.

40. A. A. P. Chazhoor, E. dmondS. L. Ho, B. Gao, and W. L. Woo, *Deep transfer learning benchmark for plastic waste classification*, Intell. Robot. **2** (2022), no. 1, 1–19.

41. H. Kim, *A low-cost compensated approximate multiplier for Bfloat16 data processing on convolutional neural network inference*, ETRI J. **43** (2021), no. 4, 684–693.

42. S. I. Khan, A. Shahrior, R. Karim, M. Hasan, and A. Rahman, *Multinet: a deep neural network approach for detecting breast cancer through multi-scale feature fusion*, J. King Saud Univers.-Comput. Inf. Sci. **34** (2022), no. 8, 6217–6228.

43. M. Elpeltagy and H. Sallam, *Automatic prediction of COVID-19 from chest images using modified ResNet50*, Multimedia Tools Appl. **80** (2021), no. 17, 26451–26463.

44. B. R. G. Elshoky, E. M. G. Younis, A. A. Ali, and O. A. S. Ibrahim, *Comparing automated and non-automated machine learning for autism spectrum disorders classification using facial images*, ETRI J. **44** (2022). https://doi.org/10.4218/etrij.2021-0097

45. N. Saleh, M. Abdel Wahed, and A. M. Salaheldin, *Transfer learning-based platform for detecting multi-classification retinal disorders using optical coherence tomography images*, Int. J. Imaging Syst. Technol. **32** (2022), no. 3, 740–752.

46. R. K. Mishra, S. Urolagin, J. A. A. Jothi, and P. Gaur, *Deep hybrid learning for facial expression binary classifications and predictions*, Image Vision Comput. **128** (2022), 104573.

47. N. Nida, M. H. Yousaf, A. Irtaza, and S. A. Velastin, *Video augmentation technique for human action recognition using genetic algorithm*, ETRI J. **44** (2022), no. 2, 327–338.

48. P. Das and D. Hussain Mazumder, *Predicting anatomical therapeutic chemical drug classes from 17 molecules properties of drugs by multi-label binary relevance approach with MLSMOTE*, (5th International Conference on Computational Biology and Bioinformatics, Bali Island, indonesia), 2021, pp. 1–7.

49. G. Madjarov, D. Kocev, D. Gjorgjevikj, and S. Džeroski, *An extensive experimental comparison of methods for multi-label learning*, Pattern Recogn. **45** (2012), no. 9, 3084–3104.

AUTHOR BIOGRAPHIES

Pranab Das is currently pursuing his Ph.D. degree from the National Institute of Technology Nagaland, India, in Computer Science & Engineering with a major area of research as bioinformatics. He received an M. tech degree from the National Institute of Technology Meghalaya, India, in 2021, a Bachelor of Engineering (BE) degree from Jorhat Engineering College, Assam, India, in 2018, and a Diploma from Assam Engineering Institute, Assam, India, in 2014, in Computer Science & Engineering. His research interests include Computational Biology and Bioinformatics, Drug Discovery and Design, Machine Learning, Data Mining, and Deep Learning. He has published several research papers in reputed journals and prestigious conferences, found online (**Link:**https://orcid.org/0000-0002-3757-4118).

Dilwar Hussain Mazumder received his B.E. and M.Tech. degree in Computer Science and Engineering from Jorhat Engineering College, Assam, India, and Rajiv Gandhi University, Arunachal Pradesh, India, in 2008 and 2012, respectively. He pursued his Ph.D. degree in Computer Science and Engineering from the National Institute of Technology Nagaland, India, in 2019. His research interests include computational methods for gene selection in cancer prediction such as biogeography-based optimizers, particle swarm optimizers, hybrid approaches, genetic algorithms, support vector machines and neural networks, data analytics, and bioinformatics with emphasis to drug discovery. He has published several research papers in reputed journals and prestigious conferences. He is having more than 15 years of experience in Teaching and Research. Currently, he is working as an Assistant Professor at the Department of Computer Science and Engineering, National Institute of Technology Nagaland, India. (**Link:**https://nitnagaland.irins.org/profile/108612).